Accepted Manuscript

The phytocannabinoid (-)-cannabidiol (CBD) operates as a complex, differential modulator of human hair growth: Anti-inflammatory submicromolar versus hair growth inhibitory micromolar effects

Imre L. Szabó, Erika Herczeg-Lisztes, Gabriella Béke, Kinga Fanni Tóth, Ralf Paus, Attila Oláh, Tamás Bíró

PII: S0022-202X(19)32558-8

DOI: https://doi.org/10.1016/j.jid.2019.07.690

Reference: JID 2027

To appear in: The Journal of Investigative Dermatology

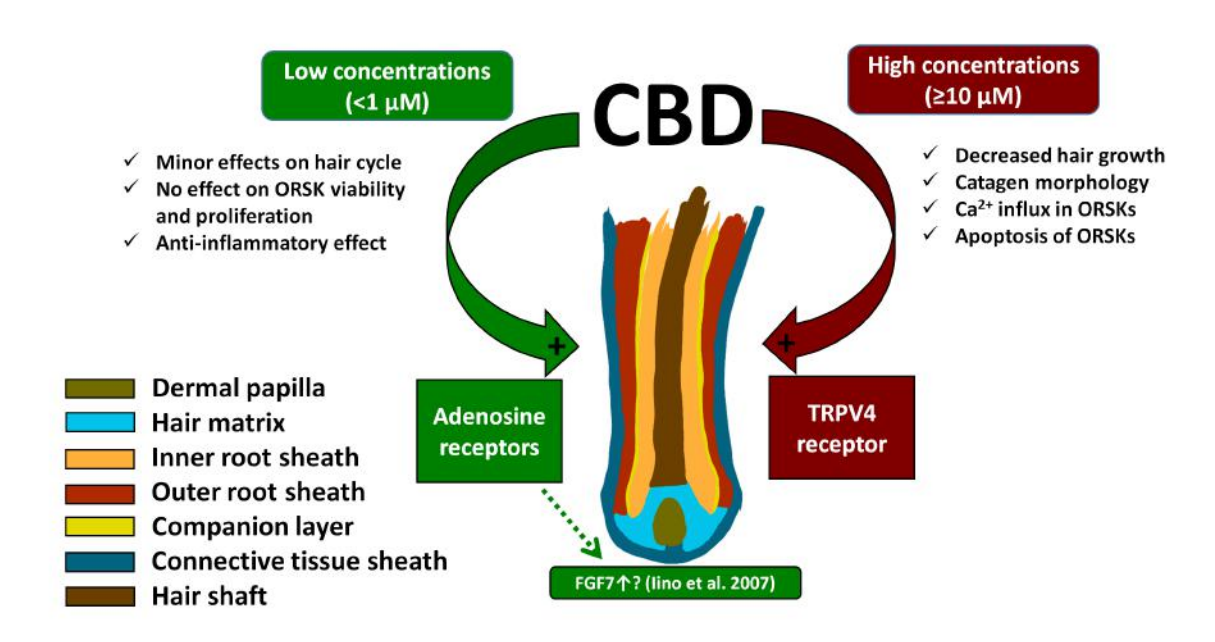
Received Date: 12 February 2019

Revised Date: 8 June 2019 Accepted Date: 2 July 2019

Please cite this article as: Szabó IL, Herczeg-Lisztes E, Béke G, Tóth KF, Paus R, Oláh A, Bíró T, The phytocannabinoid (-)-cannabidiol (CBD) operates as a complex, differential modulator of human hair growth: Anti-inflammatory submicromolar versus hair growth inhibitory micromolar effects, *The Journal of Investigative Dermatology* (2019), doi: https://doi.org/10.1016/j.jid.2019.07.690.

This is a PDF file of an unedited manuscript that has been accepted for publication. As a service to our customers we are providing this early version of the manuscript. The manuscript will undergo copyediting, typesetting, and review of the resulting proof before it is published in its final form. Please note that during the production process errors may be discovered which could affect the content, and all legal disclaimers that apply to the journal pertain.







Letter to the Editor

The phytocannabinoid (-)-cannabidiol (CBD) operates as a complex, differential modulator of human hair growth: Anti-inflammatory submicromolar versus hair growth inhibitory micromolar effects

Imre L. Szabó^{1*}, Erika Herczeg-Lisztes^{1*}, Gabriella Béke², Kinga Fanni Tóth¹, Ralf Paus^{3,4},
Attila Oláh^{1#}, Tamás Bíró^{5,6#}

¹Department of Physiology, Faculty of Medicine, University of Debrecen, Debrecen, Hungary; ²Department of Dermatology, Faculty of Medicine, University of Debrecen, Debrecen, Hungary; ³Centre for Dermatology Research, University of Manchester, MAHSC and NIHR Manchester Biomedical Research Centre, Manchester UK; ⁴Department of Dermatology & Cutaneous Surgery, University of Miami Miller School of Medicine, Miami, FL, USA; ⁵Department of Immunology, Faculty of Medicine, University of Debrecen, Debrecen, Hungary; ⁶Hungarian Center of Excellence for Molecular Medicine, Szeged, Hungary

*These authors contributed equally. #These authors contributed equally.

Word count: 1049. Number of references: 15. Number of tables: 0. Number of figures: 2.

Conflict of interest: A.O. and T.B. provide consultancy services to Botanix Pharmaceuticals Ltd. (A.O.) and Phytecs Inc. (T.B.). Botanix Pharmaceuticals Ltd., Phytecs Inc., and the founding sponsors listed in the Acknowledgements section had no role in conceiving the study, designing the experiments, writing of the manuscript, or in the decision to publish it.

Corresponding authors:

Tamás Bíró (e-mail: <u>biro.tamas@med.unideb.hu</u>; phone/FAX: +3652-417-159) and Attila Oláh (e-mail: <u>olah.attila@med.unideb.hu</u>; phone: +3652-255-575; FAX: +3652-255-116), University of Debrecen, Egyetem tér 1. Debrecen, H-4032, Hungary.

Short title: Cannabidiol differentially modulates human hair growth

Abbreviations: (-)-cannabidiol, CBD; hair cycle, HC; hair follicle, HF; toll-like receptor, TLR; transient receptor potential vanilloid-4, TRPV4.

To the editor,

Most cases of excessive hair loss and unwanted hair growth (effluvium, alopecia, hirsutism, hypertrichosis) result in part from major disturbances in the cyclic transformation of hair follicles (HFs), namely in their switch from active growth and pigmented hair shaft production (anagen) to apoptosis-driven HF involution (catagen) (Oh et al. 2016; Paus and Cotsarelis 1999). It is now clear that this switch also underlies profound neuroendocrine controls that still await systematic therapeutic targeting (Paus et al. 2014).

In this context, the endocannabinoid system is of special interest (Oláh and Bíró 2017; Tóth et al. 2019) (s1). Specifically, activation of CB₁ receptors by the endocannabinoid anandamide, and the plant-derived (-)- Δ^9 -trans-tetrahydrocannabinol, promotes premature catagen entry in human scalp HFs $ex\ vivo$ (Telek et al. 2007). Yet, 2-arachidonoylglycerol, another prototypic endocannabinoid, does not modulate HF growth $ex\ vivo$, suggesting functional heterogeneity between different cannabinoids in terms of human hair growth modulation (Telek et al. 2007).

This motivated us to also explore how another phytocannabinoid, (-)-cannabidiol (CBD), impacts on human hair growth. This major non-psychotropic phytocannabinoid does not activate CB_1 receptors, but may context-dependently signal via modulating several other targets (e.g. GPR55, 5- HT_{1a} or μ -opioid receptors, etc.) (Pertwee 2008). Moreover, it is used in the clinical practice in multiple sclerosis and certain epilepsies, and is currently under intense investigation for various uses in clinical medicine, ranging from neuropsychiatric disorders to acne (ID at ClinicalTrials.gov: NCT03573518) (s2-s5). In fact, CBD exerts complex sebostatic and anti-inflammatory effects on the pilosebaceous unit by activating both transient receptor potential vanilloid-4 (TRPV4) ion channels and adenosine A_{2A} receptors on sebocytes (Oláh et al. 2014). Topically administered CBD is likely to also reach human HFs, which express functional TRPV4 receptors whose stimulation induce premature catagen

(Szabó et al. 2018), while adenosine reportedly promotes human hair growth (Oura et al. 2008).

Therefore, we asked in the current exploratory pilot study whether and how CBD impacts on microdissected, organ-cultured human scalp HFs (Langan et al. 2015) and primary human outer root sheath keratinocytes (ORSK) isolated and cultured from plucked hair shafts (Ramot et al. 2018), obtained after written informed consent from dermatologically healthy individuals. The study adhered to Helsinki guidelines, and was institutionally and governmentally approved. For methodological details, see the **Supplementary Materials and methods** section.

First, we probed if CBD influenced hair shaft production of microdissected human HFs. We found that, when applied at 0.1 μM, CBD tended to promote hair shaft elongation, but, unexpectedly, did not modulate HF cycling and hair matrix keratinocyte proliferation or apoptosis *ex vivo* (**Figure 1**). This tendency may represent a pseudo-elongation of the hair shaft, which is pushed out of its anchorage in the HF by tissue shrinkage during the course of organ culture. Instead, 10 μM CBD significantly suppressed hair shaft production (**Figure 1a**; **Supplementary Figure S1**), and induced development of catagen morphology (**Figure 1b-c**). This was accompanied by a significant reduction of the ratio of proliferating (Ki-67+) and a significant increase in the percentage of apoptotic (TUNEL+) hair matrix keratinocytes (**Figure 1d-e**), indicating the onset of an apoptosis-associated involution. This invited the hypothesis that CBD may concentration-dependently target different receptors.

This hypothesis was probed in cultured ORSKs, which facilitate mechanistic analyses, and permit higher throughput assessments than very scarcely available scalp HFs. In line with the above HF data, CBD rapidly decreased the ORSK count (3-72-hr treatments; CyQUANT-

assay; **Supplementary Figure S2a-d**), reduced viability, and induced chiefly apoptotic cell death in a concentration- and time-dependent manner (24-hr treatments; MTT-assay and combined DilC₁(5)-SYTOX Green labeling; **Supplementary Figure S3a-b**).

CBD activates mostly Ca^{2+} -permeable TRPV4 ion channels (Oláh et al. 2014), whose stimulation promotes catagen in human HFs *ex vivo* (Szabó et al. 2018). In line with this, the catagen-promoting CBD concentration (\geq 10 μ M) induced Ca^{2+} -influx in cultured ORSKs (**Figure 2a-b**), which was almost completely abrogated by the highly selective TRPV4 antagonist, HC067047 (1 μ M) (s6). (**Figure 2c-d**). This suggests that, at micromolar concentrations, CBD activates TRPV4 in human ORSKs, and that its catagen-promoting effect on organ-cultured HFs may be stimulated via signaling through this newly identified catagen-inducing pathway.

Reportedly, toll-like receptor 3 (TLR3) activation on human ORSKs leads to inflammasome activation and subsequent interleukin (IL)-1 β production (Shin et al. 2017), which may create a pro-inflammatory, catagen- and HF dystrophy-promoting signaling milieu (s7-s9). Since CBD exerts remarkable anti-inflammatory effects in several systems (Oláh et al. 2017) (s10), we also assessed how a non-cytotoxic (Supplementary Figure S2a-d and S3a-b) and non-catagen-promoting (Figure 1a-e) CBD concentration (i.e. 0.1 μ M) impacts on the production of catagen-promoting cytokines by ORSKs. Interestingly, CBD effectively antagonized not only the TLR3-activator poly-(I:C)-induced up-regulation of *IL-1\beta*, but also that of *IL-6*, *IL-8*, and *tumor necrosis factor-\alpha (TNF-\alpha)* (Figure 2e). Similar to sebocytes, these anti-inflammatory actions of CBD appear to primarily depend on adenosine receptor-mediated signaling, since the adenosine receptor pan-antagonist CGS 15943 (s11-s13) almost completely abrogated the CBD effects reported above (Figure 2e). Besides potentially reducing the hair growth-inhibitory effects of the likely high level of these wounding-

associated cytokines of freshly microdissected HFs compared to vehicle-treated controls, the moderate hair shaft-stimulatory effects of 0.1 µM CBD (**Fig. 1a**) may also result from increased FGF7 transcription by human dermal papilla fibroblasts (Iino et al. 2007). Therefore, it deserves further dissection whether submicromolar CBD helps to normalize a catagen-promoting, pro-inflammatory HF signaling milieu, reduces the cytokine-driven recruitment and activation of hair growth-inhibitory immune cells to the HFs, and promotes the production of hair growth-supporting growth factors such as FGF7.

Although our pilot data need to be followed up by systematic dose-response experiments in a wider range of CBD concentrations, tested in HF organ cultures from additional patients, the current data invite the hypothesis that submicromolar, adenosine receptor-activating doses of CBD may reduce the intrafollicular production of catagen-promoting cytokines and could thus become useful as adjunct therapy for inflammatory hair loss disorders characterized by excessive levels of these cytokines. Instead, TRPV4-activating micromolar concentrations of CBD are attractive candidate inhibitors of unwanted hair growth (**Supplementary Figure S4**). If the current *ex vivo* findings, which imitate a systemic mode of CBD application, are reproducible after topical application, it will deserve rigorous exploration whether administering submicromolar versus micromolar topical CBD can indeed evoke differential, therapeutically desired effects in clinical hair growth management. Detailed discussion about the limitations of our study can be found in the **Supplementary Discussion** section.

ORCID

Imre Lőrinc Szabó: 0000-0002-9628-4372

Erika Herczeg-Lisztes: 0000-0002-8517-6536

Gabriella Béke: 0000-0003-3113-2287

Kinga Fanni Tóth: 0000-0002-5184-8082

Ralf Paus: 0000-0002-3492-9358

Attila Oláh: 0000-0003-4122-5639

Tamás Bíró: 0000-0002-3770-6221

Author contribution according to CRediT taxonomy:

I.L.Sz.: Investigation, Formal analysis, Project administration, Validation, Visualization, Writing – original draft, Writing – review & editing; **E.H.-L.**: Investigation, Formal analysis, Project administration, Validation, Visualization, Writing – review & editing; **G.B.**: Investigation, Project administration, Writing – review & editing; **K.F.T.**: Investigation, Project administration, Writing – review & editing; **R.P.**: Conceptualization, Writing – review & editing; **A.O.**: Conceptualization, Funding acquisition, Provision, Supervision, Writing – original draft, Writing – review & editing; **T.B.**: Conceptualization, Funding acquisition, Provision, Supervision, Writing – review & editing

Acknowledgements

This project was supported by Hungarian research grants (NKFIH 120552, 121360, and 125055; GINOP-2.3.2-15-2016-00015 "I-KOM Teaming"), and has received funding from the EU's Horizon 2020 research and innovation program under grant agreement No. 739593. AO's work was supported by the *János Bolyai Research Scholarship* of the Hungarian Academy of Sciences and by the *New National Excellence Program* of the Ministry of Human Capacities (ÚNKP-18-4-DE-247). KFT's work was supported by supported by the

Hungarian Ministry of Human Capacities (NTP-NFTÖ-18-B-0168). The authors are grateful to Dániel Bereczki and to Erika Hollósi for their technical support.

DATA AVAILABILITY STATEMENT

The data that support the findings of this study are available from the corresponding authors upon reasonable request.

References

Iino M, Ehama R, Nakazawa Y, Iwabuchi T, Ogo M, Tajima M, et al. Adenosine stimulates fibroblast growth factor-7 gene expression via adenosine A2b receptor signaling in dermal papilla cells. J. Invest. Dermatol. 2007;127(6):1318–25

Langan EA, Philpott MP, Kloepper JE, Paus R. Human hair follicle organ culture: theory, application and perspectives. Exp. Dermatol. 2015;24(12):903–11

Oh JW, Kloepper J, Langan EA, Kim Y, Yeo J, Kim MJ, et al. A Guide to Studying Human Hair Follicle Cycling In Vivo. J. Invest. Dermatol. 2016;136(1):34–44

Oláh A, Bíró T. Targeting Cutaneous Cannabinoid Signaling in Inflammation - A "High"-way to Heal? EBioMedicine. 2017;16:3–5

Oláh A, Szekanecz Z, Bíró T. Targeting Cannabinoid Signaling in the Immune System: "High"-ly Exciting Questions, Possibilities, and Challenges. Front. Immunol. 2017;8:1487

Oláh A, Tóth BI, Borbíró I, Sugawara K, Szöllősi AG, Czifra G, et al. Cannabidiol exerts sebostatic and antiinflammatory effects on human sebocytes. J. Clin. Invest. 2014;124(9):3713–24

Oura H, Iino M, Nakazawa Y, Tajima M, Ideta R, Nakaya Y, et al. Adenosine increases anagen hair growth and thick hairs in Japanese women with female pattern hair loss: a pilot, double-blind, randomized, placebo-controlled trial. J. Dermatol. 2008;35(12):763–7

Paus R, Cotsarelis G. The biology of hair follicles. N. Engl. J. Med. 1999;341(7):491–7

Paus R, Langan EA, Vidali S, Ramot Y, Andersen B. Neuroendocrinology of the hair follicle: principles and clinical perspectives. Trends Mol. Med. 2014;20(10):559–70

Pertwee RG. The diverse CB1 and CB2 receptor pharmacology of three plant cannabinoids: delta9-tetrahydrocannabinol, cannabidiol and delta9-tetrahydrocannabivarin. Br. J. Pharmacol. 2008;153(2):199–215

Ramot Y, Alam M, Oláh A, Bíró T, Ponce L, Chéret J, et al. Peroxisome Proliferator-Activated Receptor-γ-Mediated Signaling Regulates Mitochondrial Energy Metabolism in Human Hair Follicle Epithelium. J. Invest. Dermatol. 2018;138(7):1656–9

Shin J-M, Choi D-K, Sohn K-C, Kim S-Y, Min Ha J, Ho Lee Y, et al. Double-stranded RNA induces inflammation via the NF- κ B pathway and inflammasome activation in the outer root sheath cells of hair follicles. Sci. Rep. 2017;7:44127

Szabó IL, Herczeg-Lisztes E, Szegedi A, Nemes B, Paus R, Bíró T, et al. TRPV4 Is Expressed in Human Hair Follicles and Inhibits Hair Growth In Vitro. J. Invest. Dermatol. 2018;

Telek A, Bíró T, Bodó E, Tóth BI, Borbíró I, Kunos G, et al. Inhibition of human hair follicle growth by endo- and exocannabinoids. FASEB J. Off. Publ. Fed. Am. Soc. Exp. Biol. 2007;21(13):3534–41

Tóth KF, Ádám D, Bíró T, Oláh A. Cannabinoid Signaling in the Skin: Therapeutic Potential of the "C(ut)annabinoid" System. Mol. Basel Switz. 2019;24(5):918

Figure legends

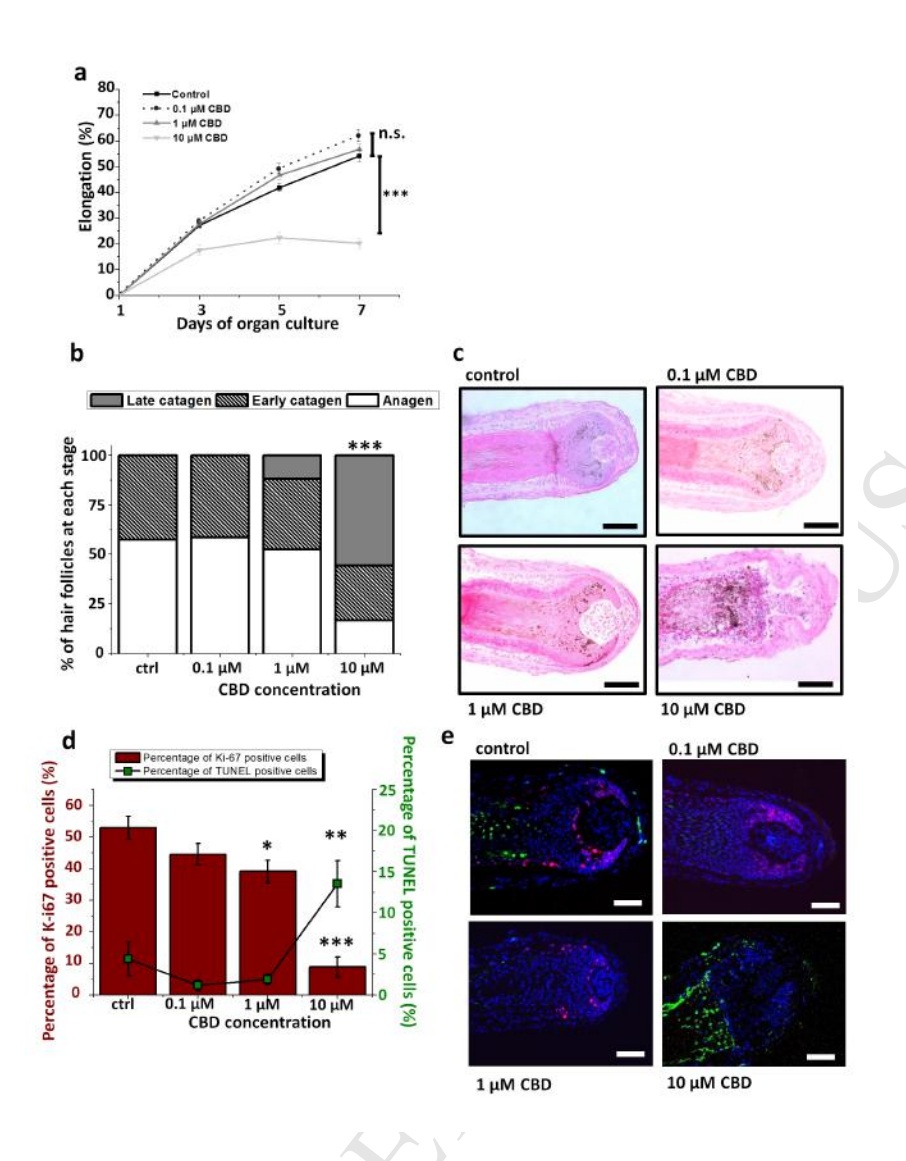
Figure 1 CBD differentially influences elongation as well as hair cycle of human microdissected hair follicles

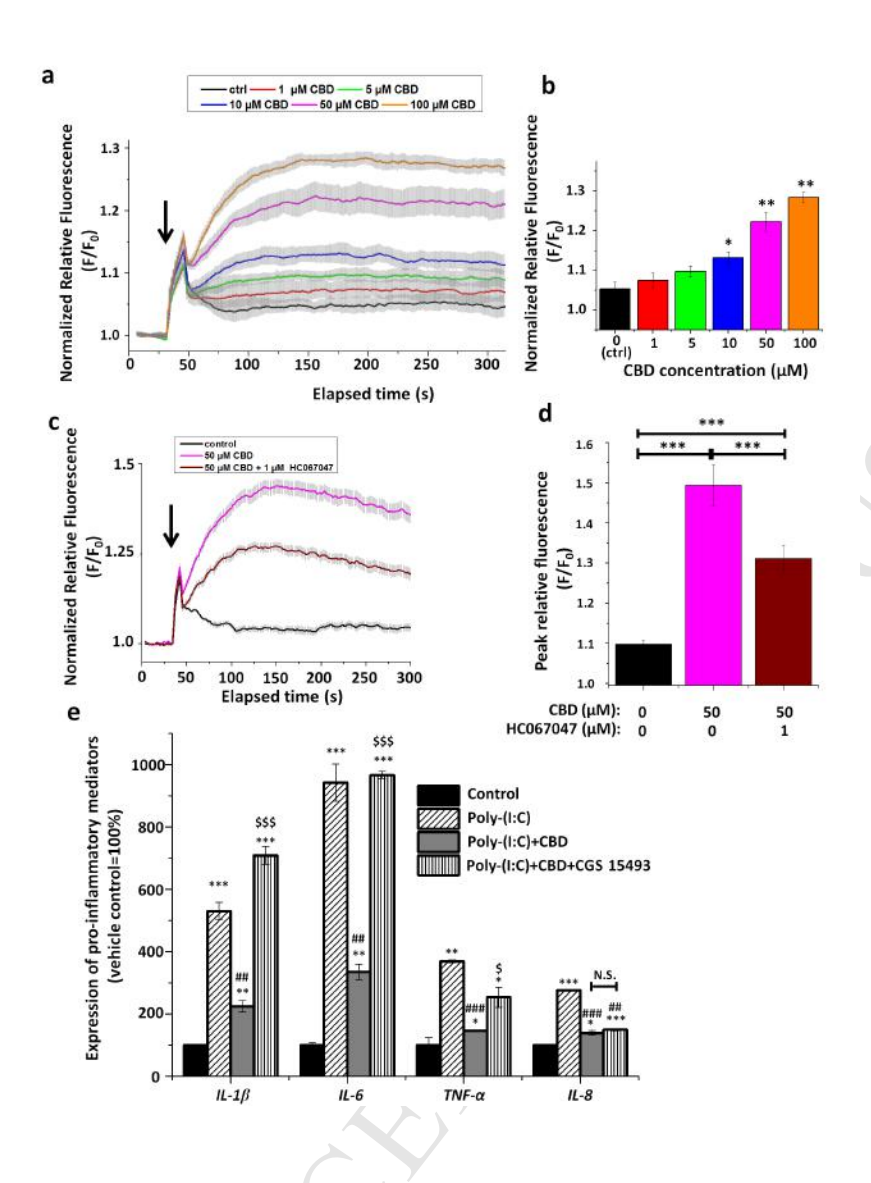
(a) Hair shaft elongation curves. HFs (N=54 HFs from 3 donors per treatment, expressed as mean±SEM) were treated as indicated. * and *** mark significant (P<0.05 and 0.001, respectively) differences as indicated at Day 7 (i.e. following 6 days of treatment). (b) Results of microscopic hair cycle staging. *** marks significant (P<0.001) differences (χ^2 -test followed by Fisher's exact test) compared to the control group. (c) Sections of representative HFs following HE staining. Scale bars: 50 µm. (d) Percentages of proliferating (Ki-67+) and apoptotic (TUNEL+) matrix keratinocytes were determined. Data are expressed as mean±SEM of N=36-40 HFs from 3 donors per treatment. *, ** and *** mark significant (P<0.05, 0.01 and 0.001, respectively) differences compared to the respective control groups. (e) Representative pictures of Ki-67 (red) and TUNEL (green) double staining after the indicated treatments. Nuclei were counterstained by 4',6-diamidino-2-phenylindole (DAPI; blue). Scale bars: 50 µm. CBD: (-)-cannabidiol; HE: hematoxylin-eosin staining; HF: hair follicle.

Figure 2 Pro-catagen concentrations of CBD activate TRPV4 ion channels, whereas at submicromolar concentration it exerts anti-inflammatory actions via the activation of adenosine receptors

(**a-d**) Fluo-4 AM-based fluorescent Ca^{2+} -measurements and their statistical analyses. Compounds were applied as indicated by the respective arrows. (**a** and **c**) Fluorescence (measured in relative fluorescence units) was normalized to the baseline, and is presented as mean \pm SEM of F/F₀ values of N=3-6 wells. (**b** and **d**) Mean \pm SEM of the peak F/F₀ values measured following the indicated treatments. *, ** and *** mark significant (P<0.05, 0.01 or 0.001, respectively) differences compared to the control (**b**) or as indicated (**d**). (**e**) Q-PCR.

TNF-α, IL-1β, IL-6, and IL-8 mRNA expression in human ORSKs was determined following the indicated 3-hr treatments (poly-(I:C): 20 μg/ml; CBD: 0.1 μM; CGS 15943: 0.1 μM). Data are presented by using ΔΔCT method regarding *GAPDH*-normalized mRNA expressions of the vehicle control as 1. Data are expressed as mean±SD of 3 determinations. Two additional experiments yielded similar results. */\$, **/##, ***/###/\$\$\$P<0.05, 0.01 or 0.001, respectively (*: vs. control; *: vs. poly-(I:C); *: vs. poly-(I:C)+CBD). n.s.: not significant. **CBD:** (-)-cannabidiol; **CGS 15943:** a pan-antagonist of the adenosine receptors; **HC067047:** specific TRPV4 antagonist; **IL:** interleukin; **poly-(I:C):** polyinosinic-polycytidylic acid (Toll-like receptor 3 activator); **TNF:** tumor necrosis factor.





SUPPLEMENTARY MATERIALS AND METHODS

Materials

(-)-cannabidiol (CBD), TRPV4-selective antagonist HC067047 (s5)the (http://www.guidetopharmacology.org/GRAC/LigandDisplayForward?tab=biology&ligandId pan-antagonist 15943 (**s10-s12**; =4213),and the adenosine receptor **CGS** http://www.guidetopharmacology.org/GRAC/LigandDisplayForward?ligandId=384) purchased from Tocris (Bristol, UK), whereas the TLR3 activator dsRNA polyinosinicpolycytidylic acid (poly-(I:C)) was obtained from Sigma-Aldrich (St Louis, MO, USA). CBD was dissolved in absolute ethanol, whereas the solvent of HC067047 and CGS 15943 was dimethyl sulfoxide (DMSO). Poly-(I:C) was dissolved in filtered distilled water. Control cultures were always treated with appropriate amount of vehicle(s).

Isolation and maintenance of HFs

Human skin samples were obtained following obtaining written informed consent from healthy individuals undergoing dermatosurgery. The study adhered to Helsinki guidelines, and was institutionally and governmentally approved by the Institutional Research Ethics Committee and the Government Office for Hajdú-Bihar County (protocol No.: DE OEC RKEB/IKEB 3724-2012; document IDs: IX-R-052/01396-2/2012, IF-12817/2015, IF-1647/2016, IF-778-5/2017). Human anagen VI HFs were isolated from skin obtained from two male (28 and 32 years old) and one female (58 years old) patients undergoing neurosurgical intervention as described before (Borbíró et al. 2011; Langan et al. 2015; Oláh et al. 2016b). Isolated HFs were cultured in Williams' E medium (Invitrogen, Paisley, UK) supplemented with 2 mM L-glutamine (Invitrogen), 10 ng/ml hydrocortisone, 10 mg/ml insulin, and antibiotics (all from Sigma- Aldrich). Treatments were initiated 24 hours after the isolation. Medium was changed every other day, whereas treatment with CBD (or vehicle)

was performed daily. Length measurements were performed on individual HFs using a light microscope with an eyepiece measuring graticule.

Isolation and culture of outer root sheath keratinocytes (ORSKs)

Isolation and culture of ORSKS was performed following our previously optimized protocols (see e.g. Borbíró et al. 2011; Ramot et al. 2018). Briefly, plucked hair shafts of healthy volunteers (both females and males; age: 23-47 years old) were digested using trypsin to isolate ORSKs. Isolated ORSKs were seeded to a feeder layer of primary human dermal fibroblasts (HDFs) that were pre-treated overnight with mitomycin C (0.4 µg/ml [from Sigma-Aldrich]) in order to block their proliferation. HDFs were obtained from deepidermized dermis using enzymatic digestion. Co-cultures of non-proliferating feeder HDFs and ORSKs were maintained in a 1:3 mixture of Ham's F12 and DMEM (both from Invitrogen) supplemented with 0.1 nM cholera toxin, 5 mg/ml insulin, 0.4 mg/ml hydrocortisone, 2.43 mg/ml adenine, 2 nM triiodothyronine, 10 ng/ml epidermal growth factor, 1 mM ascorbyl-2-phosphate and antibiotics (all from Sigma-Aldrich). ORSKs were plated for subsequent experiments on collagen-coated (1%; 37°C for 1 hour; obtained from Sigma-Aldrich) culture dishes without HDF feeder layer.

Hematoxylin-eosin (HE) staining of frozen tissue sections

6 μm thick cryosections of the HFs were dried at room temperature (10 min), and fixed in precooled acetone (10 min at -20°C). Sections were then washed in distilled water for 1 min at room temperature, and stained with Mayer's hematoxylin for 35 sec at room temperature. Following gentle washing under the tap water for 15 min at room temperature, sections were stained with 0.1% Eosin Y Solution (1 min at room temperature). Sections were then dehydrated (washing 3-4 times in 70, 96 and 100% ethanol), and incubated in Xylene (2x10 min at room temperature). Finally, sections were mounted by using Eukitt quick-hardening

mounting medium (Sigma-Aldrich). Images were taken by using bright field function of a Nikon Eclipse E600 microscope (Nikon, Tokyo, Japan). HE staining was then used for studying HF morphology, and, together with Ki-67/TUNEL double labeling (see below), for staging hair cycle to anagen, early catagen and late catagen according to pre-defined objective morphological criteria (Kloepper et al. 2010).

Assessment of proliferation and apoptosis of matrix keratinocytes (Ki-67/TUNEL double labeling)

Proliferation and apoptosis were assessed by Ki-67/TUNEL double-immunostaining as described previously (Kloepper et al., 2010; Borbíró et al. 2011; Oláh et al. 2016b). Briefly, cryosections (6 µm) were air dried for 10 minutes at room temperature (RT), and then fixed for 10 min in 1% paraformaldehyde (PFA) in phosphate-buffered saline solution (PBS; 15 mM NaCl, 20 mM Na₂HPO₄, pH 7.4; all from Sigma-Aldrich) at RT. Samples were rehydrated in PBS for 5 minutes (2x), and were then post-fixed for 5 minutes in precooled ethanol-acetic acid 2:1 at -20°C, and then rehydrated in PBS again for 5 minutes (3x). After rehydration, sections were incubated with an equilibration buffer for 5 minutes at RT, and then incubated with TdT-Enzyme for 1 hour at 37°C. To reveal proliferation, mouse antihuman Ki-67 (DAKO, Carpinteria, CA, USA) primary antibody was used. In addition, to assess apoptosis, a TUNEL assay was performed using an ApopTag Fluorescein in situ Apoptosis Detection Kit (Merck Millipore) following the manufacturer's instructions. Sections were incubated with the primary antibody overnight at 4°C, and then with the secondary antibody (Alexa Fluor 568 goat anti-mouse IgG, Invitrogen) for 45 min at RT. Sections were washed in PBS and were counterstained with 4',6-diamidino-2-phenylindole (DAPI) (Sigma-Aldrich) and mounted with Fluoromont G (Southern Biotechnology Associates, Birmingham, AL, USA). Visualization of the signals was performed by using a Nikon Eclipse E600 fluorescent microscope (Nikon). Ratio of proliferating (Ki-67+) and

apoptotic (TUNEL+) cells was determined in defined reference regions of the hair bulb, and were expressed as percentage of the total cell count determined by counting DAPI-positive nuclei.

Quantitative real-time polymerase chain reaction (Q-PCR)

Q-PCR was performed on a Stratagene MXP3005p detection system (Agilent Technologies, Santa Clara, California, USA) by using the 5' nuclease assay, as we have previously (Oláh et al. 2014). Briefly, ORSKs were seeded to Petri-dishes (d=35 mm; 500,000 cells/1.5 mL medium/dish), and were harvested following the indicated 3-hr treatments. Total RNA was then isolated using TRIzol reagent (Invitrogen) according to manufacturer's protocol. The concentrations and purities of the RNA samples were measured by NanoDrop ND-1000 spectrophotometer (Thermo Scientific, Bioscience, Budapest, Hungary), and samples were kept at -20°C until further processing. Next, DNase treatment was performed according to the manufacturer's protocol, and then, 3 µg of total RNA was reverse-transcribed into cDNA using High-Capacity cDNA Kit from Life Technologies Hungary Ltd. PCR amplification was performed using the TaqMan[®] Gene Expression Assays (assay IDs: Hs00174092 m1 for interleukin [IL]-1α; Hs00985639_m1 for IL-6; α Hs00174103_m1 for IL-8; Hs00174128_m1 for tumor necrosis factor- α [TNF- α]) and the TaqMan universal PCR master mix protocol (Applied Biosystem). As internal control, transcripts of glyceraldehyde 3-phosphate dehydrogenase [GAPDH] (assay ID Hs99999905_m1) were determined. The amount of the transcripts was normalized to those of the housekeeping gene using the Δ CT method, and then the relative expression values were further normalized to the ones of the vehicle-treated control ($\Delta\Delta$ CT method).

Fluorescent Ca²⁺ measurements

ORSKs were seeded in 96-well black-well/clear bottom plates (Greiner Bio-One, Kremsmuenster, Austria) previously coated with 1% collagen in ORSK medium at a density of 20,000 cells per well, and were incubated at 37°C for 24 hours. The cells were washed once with 1(g/100 mL)% bovine serum albumin and 2.5 mM probenecid (both from Sigma-Aldrich) containing Hank's solution (136.8 mM NaCl, 5.4 mM KCl, 0.34 mM Na₂HPO₄, 0.44 mM KH₂PO₄, 0.81 mM MgSO₄, 1.26 mM CaCl₂, 5.56 mM glucose, 4.17 mM NaHCO₃, pH 7.2, all from Sigma-Aldrich), and then were loaded with 1 µM Fluo-4 AM (Life Technologies Hungary Ltd.) dissolved in Hank's solution (100 µl/well) at 37°C for 30 min. The cells were then washed three times with Hank's solution (100 µl/well). The plates were then placed into a FlexStation II³⁸⁴ multi-mode microplate reader (Molecular Devices, Sunnyvale, CA, USA) and alterations of the cytoplasmic Ca²⁺ concentration (reflected by changes in fluorescence; λ_{EX} : 490 nm, λ_{EM} : 520 nm) were monitored at room temperature following the application of the indicated substances or vehicle. In order to probe reactivity and viability of the cells, at the end of each measurement, 0.2 mg/ml ATP was administered as a positive control (data not shown). Data are presented as F/F₀, where F₀ is the average baseline fluorescence (i.e. before compound application), whereas F is the actual fluorescence.

Determination of cellular proliferation

The degree of cellular growth (reflecting proliferation) was determined by measuring the DNA content of cells using CyQUANT Cell Proliferation Assay Kit (Life Technologies Hungary Ltd). ORSKs (5,000 cells per well) were cultured in 96-well "black well/clear bottom" plates (Greiner Bio-One), and were treated as indicated in octuplicates. Supernatants were then removed by blotting on paper towels, and the plates were subsequently frozen at -80°C. The plates were then thawed at room temperature, and 200 µl of CyQUANT dye/cell lysis buffer mixture was added to each well. After 5 min of incubation, fluorescence was

measured at 490 nm excitation and 520 nm emission wavelengths using FlexStation II³⁸⁴ multi-mode microplate reader (Molecular Devices). Relative fluorescence values were expressed as percentage of the daily vehicle control regarded as 100%.

Evaluation of cellular viability

To assess the effect on viability, we applied MTT-assay (Sigma-Aldrich) as mitochondrial enzymes of living cells are able to transform tetrazolium salt (MTT) into formazan crystals. ORSKs were seeded in 96-well plates (density: 10,000 cells/well) and were treated as indicated in octuplicates with various concentrations of CBD or vehicle. Cells were then incubated with 0.5 mg/ml MTT reagent for 3 hours, and concentration of formazan crystals (as an indicator of number of viable cells) was determined colorimetrically at 565 nm by using FlexStation 3 multi-mode microplate reader (Molecular Devices). Results were expressed as percentage of vehicle control regarded as 100%.

Determination of apoptosis

A decrease in the mitochondrial membrane potential is one of the earliest markers of apoptosis (Green and Reed, 1998, Susin et al. 1998). Therefore, to assess the process, mitochondrial membrane potential of SZ95 sebocytes was determined using a MitoProbeTM DilC₁(5) Assay Kit (Life Technologies Hungary Ltd.). Cells (10,000 cells/well) were cultured in 96-well "black well/clear bottom" plates (Greiner Bio One) in octuplicates and were treated as indicated. After removal of supernatants, cells were incubated for 30 minutes with 1,1′,3,3,3′,3′-hexamethylindodicarbo-cyanine iodide (DilC₁(5)) working solution (50 μl/well), then washed with PBS, and the fluorescence of DilC₁(5) was measured at 630 nm excitation and 670 nm emission wavelengths using FlexStation II³⁸⁴ multi-mode microplate reader (Molecular Devices). Relative fluorescence values were expressed as percentage of vehicle control regarded as 100%.

Determination of necrosis

Necrotic processes were determined by SYTOX Green staining (Life Technologies Hungary Ltd.). The dye is able to penetrate (and then to bind to the nucleic acids) only to necrotic cells with ruptured plasma membranes, whereas healthy cells with intact surface membranes show negligible SYTOX Green staining intensity. Cells were cultured in 96-well "black well/clear bottom" plates (Greiner Bio One), and treated as indicated. Supernatants were then discarded, and the cells were incubated for 30 minutes with 1 μM SYTOX Green dye. Following incubation, cells were washed with PBS, the culture medium was replaced, and fluorescence of SYTOX Green was measured at 490 nm excitation and 520 nm emission wavelengths using FlexStation II³⁸⁴ multi-mode microplate reader (Molecular Devices). Relative fluorescence values were expressed as percentage of negative control regarded as 100%. Due to their spectral properties, DilC₁(5) and SYTOX Green dyes were always administered together, enabling us to investigate necrotic and early apoptotic processes of the same cultures. Selective decrease of DilC₁(5) intensity indicated mitochondrial depolarization (i.e. the onset of early apoptotic processes), whereas increase of SYTOX Green staining intensity revealed necrotic cell death.

Statistical analysis

When applicable, data were analyzed using Origin Pro Plus 6 software (Microcal, Northampton, MA, USA) using χ^2 -test followed by Fisher's exact test, Student's two-tailed unpaired *t*-test, or ANOVA with Bonferroni *post hoc* test and P<0.05 values were regarded as significant differences.

DATA AVAILABILITY STATEMENT

The data that support the findings of this study are available from the corresponding authors upon reasonable request.

SUPPLEMENTARY DISCUSSION – Limitations of our study

When interpreting the results presented in the current exploratory, pilot study, one has to keep in mind that, while it sheds light to previously unknown and hair-wise potentially relevant dermatological effects of CBD, the current work has certain important limitations as well.

First and foremost, as mentioned in the main text, our data need to be followed up by systematic dose-response experiments in a wider range of CBD concentrations, tested in HF organ cultures from additional patients to explore existence and magnitude of inter-donor variability.

Second, by adding CBD (or vehicle) to the culture medium, in the current study, we mimicked the effects of systematically administered CBD. However, from a translational point-of-view, it will be crucially important to assess biological effects of CBD following standardized topical application in appropriate formulations.

Third, it is important to emphasize that in the current study, we used microdissected, truncated HFs lacking the bulge region as well as other (non-HF) members of the pilosebaceous unit (namely the sebaceous glands and the arrector pili muscles). Therefore, we cannot exclude the possibility that specific (and most likely concentration-dependent) actions of CBD on these structures may influence the production and release of hair cycle-regulating substances, further modifying thereby its already quite complex effects on the hair cycle.

Fourth, studying microdissected HFs *ex vivo* has the inherent limitation of missing the effects and regulatory roles of intact innervation and blood supply. This may be crucially important, since it can lead to model-dependently opposing observations in certain cases. Indeed, in case of e.g. the TRPV1-activating capsaicin, we have previously shown that it suppressed hair growth and induced premature catagen entry in microdissected human hair follicles (Bíró et al. 2006). Moreover, lack of TRPV1 in KO animals delayed their normal hair cycle (Bodó et al. 2005). However, administration of capsaicin was found *to promote* hair growth by increasing insulin-like growth factor-I production in mice and in humans with alopecia, most

likely via acting on sensory nerve fibers (Harada et al. 2010). Given the broad target spectrum of CBD, one can speculate that it may also modulate production and release of hair cycle-regulator substances from sensory nerve endings, therefore its impact on human hair biology may be even more complex.

SUPPLEMENTARY FIGURE LEGENDS

Supplementary Figure S1 *Macroscopic appearance the HFs following the indicated CBD-or*

vehicle treatments (representative images)

CBD: (-)-cannabidiol.

Supplementary Figure S2 CBD concentration and time-dependently decreases cell count of

ORSKs

(a-d) CyQUANT-assays. ORSKs were plated at low (5,000/well) initial cell count to enable

rapid proliferation. Cell count was assessed following 3 (a), 24 (b), 48 (c) and 72-hr (d)

treatments. Results are expressed in the percentage of the daily vehicle control as mean±SEM

of eight independent determinations. Two additional experiments yielded similar results. ***

marks significant (P<0.001) difference compared to the respective control group.

CBD: (-)-cannabidiol.

Supplementary Figure S3 High CBD concentrations reduce viability, and induce apoptosis-

dominated cell death

ORSKs were treated as indicated for 24 hours, and viability (a) as well as cell death (b) were

assessed by MTT-assay and combined DilC₁(5)-SYTOX Green labeling, respectively. Results

are expressed in the percentage of the vehicle control as mean±SEM of eight independent

determinations. Two additional experiments yielded similar results. ** and *** mark

significant (P<0.01 or 0.001, respectively) differences compared to the respective control

group. **CBD:** (-)-cannabidiol.

Supplementary Figure S4 Overview of the effects of CBD: CBD differentially influences

human hair follicle biology in a concentration-dependent manner

10

High (≥10 µM) concentrations of CBD induced premature catagen entry via activating TRPV4 ion channels expressed on the outer root sheath keratinocytes (ORSKs). Importantly, such pro-catagen effect of TRPV4 is not unprecedented, since it has recently been demonstrated that activation of this channel, similar to that of the structurally closely related TRPV3 (Borbíró et al. 2011) and TRPV1 (Bíró et al. 2006; Bodó et al. 2005), is a potent inducer of catagen transformation of human HFs (Szabó et al. 2018). Intriguingly, however, when applied at low, sub-micromolar concentrations, CBD tended to promote hair shaft production. Although in light of the unaltered proliferation and apoptosis rates, this may represent a pseudo-elongation of the hair shaft, which is pushed out of its anchorage in the HF by tissue shrinkage during the course of organ culture, our data indicate that submicromolar concentrations of CBD may exert differential effect on human HFs. Indeed, 0.1 µM CBD prevented the TLR3-activator poly-(I:C)-induced up-regulation of several pro-inflammatory cytokines in cultured ORSKs in an adenosine receptor-dependent manner, since the adenosine receptor pan-antagonist CGS 15943 (0.1 µM) could almost completely abrogate this effect. Although exploration of the adenosine receptor expression profile of human HFs is beyond the scope of the current letter, these data suggest that, besides the ones expressed on the dermal papilla cells (Iino et al. 2007), adenosine receptors of the ORSKs are also functionally active, and may contribute to the regulation of hair cycle, as well as of other aspects of HF biology. Obviously, it remains to be dissected in future targeted studies if moderate hair shaft production-promoting effects of low CBD concentrations are coupled to the A2B receptordependent up-regulation of FGF7 expression in the dermal papilla (Iino et al. 2007), or are rather mediated in an ORSK-dependent manner, or the two pathways complement each other.

SUPPLEMENTARY REFERENCES (appearing in the main text)

- s1 Maccarrone M, Bab I, Bíró T, Cabral GA, Dey SK, Di Marzo V, et al. Endocannabinoid signaling at the periphery: 50 years after THC. Trends Pharmacol. Sci. 2015;36(5):277–96
- **s2** Chelliah MP, Zinn Z, Khuu P, Teng JMC. Self-initiated use of topical cannabidiol oil for epidermolysis bullosa. Pediatr Dermatol. 2018;35(4):e224–7
- s3 Crippa JA, Guimarães FS, Campos AC, Zuardi AW. Translational Investigation of the Therapeutic Potential of Cannabidiol (CBD): Toward a New Age. Front Immunol. 2018;9:2009
- **s4** Pisanti S, Malfitano AM, Ciaglia E, Lamberti A, Ranieri R, Cuomo G, et al. Cannabidiol: State of the art and new challenges for therapeutic applications. Pharmacol. Ther. 2017;175:133–50
- s5 Armstrong JL, Hill DS, McKee CS, Hernandez-Tiedra S, Lorente M, Lopez-Valero I, et al. Exploiting cannabinoid-induced cytotoxic autophagy to drive melanoma cell death. J. Invest. Dermatol. 2015;135(6):1629–37
- s6 Everaerts W, Zhen X, Ghosh D, Vriens J, Gevaert T, Gilbert JP, et al. Inhibition of the cation channel TRPV4 improves bladder function in mice and rats with cyclophosphamide-induced cystitis. Proc. Natl. Acad. Sci. U.S.A. 2010;107(44):19084–9
- **s7** Hoffmann R, Happle R, Paus R. Elements of the interleukin-1 signaling system show hair cycle-dependent gene expression in murine skin. Eur J Dermatol. 1998;8(7):475–7
- **s8** Philpott MP, Sanders DA, Bowen J, Kealey T. Effects of interleukins, colony-stimulating factor and tumour necrosis factor on human hair follicle growth in vitro: a possible role for interleukin-1 and tumour necrosis factor-alpha in alopecia areata. Br. J. Dermatol. 1996;135(6):942–8
- **s9** Rückert R, Lindner G, Bulfone-Paus S, Paus R. High-dose proinflammatory cytokines induce apoptosis of hair bulb keratinocytes in vivo. Br. J. Dermatol. 2000;143(5):1036–9
- **s10** Esposito G, Filippis DD, Cirillo C, Iuvone T, Capoccia E, Scuderi C, et al. Cannabidiol in inflammatory bowel diseases: a brief overview. Phytother Res. 2013;27(5):633–6
- **s11** Ghai G, Francis JE, Williams M, Dotson RA, Hopkins MF, Cote DT, et al. Pharmacological characterization of CGS 15943A: a novel nonxanthine adenosine antagonist. J. Pharmacol. Exp. Ther. 1987;242(3):784–90
- **s12** Klotz KN, Adenosine receptors and their ligands. Naunyn Schmiedebergs Arch. Pharmacol. 2000;362(4–5):382–91
- **s13** Williams M, Francis J, Ghai G, Braunwalder A, Psychoyos S, Stone GA, et al. Biochemical characterization of the triazoloquinazoline, CGS 15943, a novel, non-xanthine adenosine antagonist. J. Pharmacol. Exp. Ther. 1987;241(2):415–20

SUPPLEMENTARY REFERENCES (appearing only in the supplementary section)

- Bíró T, Bodó E, Telek A, Géczy T, Tychsen B, Kovács L, et al. Hair cycle control by vanilloid receptor-1 (TRPV1): evidence from TRPV1 knockout mice. J. Invest. Dermatol. 2006;126(8):1909–12
- Bodó E, Bíró T, Telek A, Czifra G, Griger Z, Tóth BI, et al. A hot new twist to hair biology: involvement of vanilloid receptor-1 (VR1/TRPV1) signaling in human hair growth control. Am. J. Pathol. 2005;166(4):985–98
- Borbíró I, Lisztes E, Tóth BI, Czifra G, Oláh A, Szöllosi AG, et al. Activation of transient receptor potential vanilloid-3 inhibits human hair growth. J. Invest. Dermatol. 2011;131(8):1605–14
- Green DR, Reed JC. Mitochondria and apoptosis. Science. 1998;281(5381):1309-12
- Harada N, Okajima K, Arai M, Kurihara H, Nakagata N. Administration of capsaicin and isoflavone promotes hair growth by increasing insulin-like growth factor-I production in mice and in humans with alopecia. Growth Horm. IGF Res. 2007;17(5):408–15
- Kloepper JE, Sugawara K, Al-Nuaimi Y, Gáspár E, Beek NV, Paus R. Methods in hair research: how to objectively distinguish between anagen and catagen in human hair follicle organ culture. Experimental Dermatology. 2010;19(3):305–12
- Oláh A, Gherardini J, Bertolini M, Chéret J, Ponce L, Kloepper J, et al. The Thyroid Hormone Analogue KB2115 (Eprotirome) Prolongs Human Hair Growth (Anagen) Ex Vivo. J. Invest. Dermatol. 2016b;136(8):1711–4
- Susin SA, Zamzami N, Kroemer G. Mitochondria as regulators of apoptosis: doubt no more. Biochim Biophys Acta. 1998;1366(1-2):151-165

